University of California
Santa Barbara

Design of a Soft Continuum Sensor Utilizing Macrobend Losses of Optical Fibers

A thesis submitted in partial satisfaction
of the requirements for the degree

Master of Science
in
Mechanical Engineering

by

Patrick Corrigan Curtis

Committee in charge:

Professor Elliot Hawkes, Chair
Professor Megan Valentine
Professor Igor Mezić

June 2021

The Thesis of Patrick Corrigan Curtis is approved.

Professor Megan Valentine

Professor Igor Mezić

Professor Elliot Hawkes, Committee Chair

June 2021

This page was left intentionally blank.

Acknowledgements

The author would like to acknowledge my advisor, Professor Elliot Hawkes, and committee members Professors Megan Valentine and Igor Mezić, for overseeing this project. I would like to give a special thanks to Professor Mike Gordon for his generosity with his equipment, lab space, expertise, and time, and without whom this project would not have been possible.

I would also like to thank my collaborators David Haggerty and Michael Banks, who were a pleasure to work with and learn from.

Additionally, I would like to thank the National Science Foundation for funding the EFRI C3 SoRo project at UC Santa Barbara, this work would have never happened without them.

Lastly, I would like to express my deepest gratitude to the faculty and staff of UC Santa Barbara that played a role in keeping the campus safe and open for research during the COVID-19 Pandemic. This would not have been possible without them.

Curriculum Vitæ

Patrick Corrigan Curtis

Education

2021	M.S. in Mechanical Engineering (Expected), University of California, Santa Barbara.
2019	B.S. in Mechanical Engineering, B.A. in German, University of Rhode Island

Publications

Modeling, Reduction, and Control of a Helically Actuated Inertial Soft Robotic Arm via the Koopman Operator

Abstract

Design of a Soft Continuum Sensor Utilizing Macrobend Losses of Optical Fibers

by

Patrick Corrigan Curtis

When compared with traditional robotic manipulators that use discrete rigid links and discrete joints, the sensing of soft robotic manipulators is inaccurate and their control is clumsy. This is because that the orientation of a traditional robotic arm can be known sufficiently by measuring relative rotation and translation of the links and joints subject to some initial condition. This could be done by implementing rotary encoders at every joint in a traditional rigid manipulator. Because of their continuum nature, a soft robotic arm's orientation can only be known exactly if an infinite number were to be used. Therfore, the orientation of soft robotic manipulators can only be practically described when applying a set of simplifying assumptions such as piecewise-constant curvature. There are many ways to obtain information that can be used to describe the curvature of a soft robot; Motion capture is a prevailing technique in research but require that the robot is confined to spaces where motion capture can be used. Since this is not possible in many promising applications of soft robotics, including but not limited to minimally invasive surgery and disaster site navigation, many are looking to other ways to make robots capable of proprioception without using external sensors. One option is incorporating fiber optic sensing into soft robots. Fiber is flexible and a staggering amount of information about a system can be determined by reading changes in wavelength, phase shift, etc, which makes it an excellent solution for soft systems. The problem with incorporating fiber optics into soft robotics is that equipment and technologies such as optical spectrum analyzers, interrogators, fiber Bragg gratings are prohibitively expensive. Some work has been done

showcasing that the optical intensity transmitted through a fiber can be correlated with the deformation that the fiber is experiencing (also known as macrobend loss or fiber optic intensity modulation), which can be read with much more accessible equipment. While promising, existing research only uses this technique to measure axial strain. We propose extending the method to determine arbitrary shapes of a continuum arm. We believe the power of data-driven methods will allow us to glean enough information from bending loss to achieve shape reconstruction currently only possible with high-cost optical spectrum analyzers. Specifically, this work aims to use a data-driven method to link the pose of a flexible arm with the intensity outputs of a number of fiber optic sensors attached to its body, using motion capture as ground truth. This work serves as the groundwork necessary for establishing a new low-cost optical sensing technique for soft robotics that could potentially allow important advancements in sensing and thus control.

Contents

Chapter 1

Introduction

Many works have investigated the use of fiber optics as a platform for strain and pressure sensing. The state-of-the-art technology usually relies on the use of spectrometry and interferometry of an incident fiber optic signal subjected to various stimuli. Most of these strategies are highly cost-prohibitive and therefore not amenable for adoption in soft robotic platforms. Some work has been done to investigate the effect of stimuli such as bending or compression on the bending losses of optical fiber. This is a counter-intuitive idea, since the motivation behind using fiber optics in a more conventional sense is that hardly any data is lost due to total internal reflection of incident light. The principle is remarkably simple; a fiber optic cable has a specified minimum bending radius, when it has bends that are smaller than this radius, the angle of incidence at the core-cladding interface is high enough to overcome the difference in refraction index and the light will escape to the cladding and eventually, out of the fiber entirely. The macrobend loss of an optical fiber is a function of the tightness and number of turns that the optical fiber makes. For this investigation, the fiber was woven into a 3D-printed mold that had pegs on opposing sides spaced 1.5cm apart along the axis of the mold. The mold was filled with Smooth-on Dragonskin 10 silicone and cured in an oven at 70C until firm. The

result was a thin, compliant sensor consisting of fibers encapsulated in silicone, making a device that can be easily integrated into a soft robotic platform.

1.1 Motivation

This investigation was inspired by previous work, using motion capture to obtain ground truth data for a soft robotic arm in experiments for Modeling, Reduction, and Control of a Helically Actuated Inertial Soft Robotic Arm via the Koopman Operator [1]. Motion capture is a robust and convenient tool for research, but it is not a feasible sensing solution for soft robots deployed in real-life scenarios, especially ones where the soft robot may be traversing long distances. This prompted thinking on how the pose and curvature of a soft manipulator could be measured continuously without relying solely on motion capture. During investigation, numerous papers utilizing the output of optical fibers were found. The state-of-the-art in fiber optic based sensing can obtain sophisticated information about a soft robotic manipulator such as high-resolution shape sensing, environmental mapping, and material stiffness property by utilizing optical frequency domain reflectometry (OFDR) [2]. This shows tremendous promise, however a fiber optic sensing system from Luna Innovations, Inc is utilized in this paper; which is an incredibly useful and robust platform but also prohibitively expensive (some interrogators are in excess of 100,000 USD). One alternative to OFDR for soft robotic sensing is fiber optic intensity modulation (FOIM), where losses in optical intensity being transmitted through a fiber optic cable is correlated with some stimuli. One paper found that a fiber embedded sinusoidally in a silicone gripper equipped with fiber Bragg gratings showed substantially more attenuation in the signal reflected by the gratings when subjected to bending or grasping an object than a fiber that was embedded in a straight manner (additionally, the fiber, being rather inextensible, embedded in a straight manner often

delaminated in the highly elastic silicone) [3]. The results of this paper were promising, but fiber Bragg gratings require specialized equipment and expertise to produce, and detecting the power of a reflected signal. Another approach utilizing optical power losses to measure deformation in soft systems was seen in To, et al where gold waveguide deposited onto a flexible PDMS substrate was coupled with a fiber emitting an IR signal through the waveguide. The optical power losses were caused by microcracks in the sputtered gold which grew in size as the material was stretched [4]. Another paper, by Sareh et al, explores the use of microbend losses in fiber optics in order to get a pose estimation of a 3-DOF soft robotic arm [5]. The sensing principle employs only the optical intensity via a photodiode and is therefore a "single-pixel" measurement of the macrobend losses. A low-cost sensor that uses macrobend losses to measure axial displacement has been shown to work [6], laying the groundwork for a similar sensor to work in other modes of strain. In the experiment performed in subsequent sections, it was then surmised that there is more information encoded in the distribution of the fiber optic output. In order to implement a larger number of parameters that may contain information key to reconstructing the pose of this experiment's soft arm from data, the output from the fibers was collected by pointing their ends at a camera and recording how the output changes. Lastly, a paper by Truby et al investigates the use of machine learning to perform distributed proprioception on a soft robotic arm not dissimilar from our own [7]. This device utilized different resistive sensors along the body of the robot. Their outputs were nonlinear and hysteretic, so a machine learning algorithm was developed to map the output of the sensors to the robot pose that was also obtained with motion capture. This paper made a constant-curvature assumption for each of the sections, but their idea of using a series of sensors along the axis of a soft arm to estimate its pose is analogous to the ultimate goal of the work presented in this investigation, with the attenuation of light being used to estimate the pose instead of a voltage drop. Ultimately, this investigation

aims to use the signal information to estimate an arbitrary superposition of curvatures in a soft continuum, and will not attempt at a reconstruction based on a constant-curvature assumption.

Chapter 2

Device Design

2.1 Soft Sensor Design

For the purpose of this paper, the arm is not capable of self actuation. It is merely a device that is used to demonstrate the capability of the macrobend fiber-optic sensor when subjected to in-plane bending. Incorporating actuation into this device may be added in the future but the primary focus here is to demonstrate this as a viable sensing solution. This section details the construction of the fiber-optic sensor and the factors that went into iterative changes. Two different types of optical fiber were used in this experiment, 250-micron diameter FG105LVA multimode fiber from ThorLabs, and an unjacketed generic PMMA fiber of the same diameter. Fibers were woven through a 3D-printed mold as seen in Figure 2.1.

The 1.5cm spacing of the mold pegs were to ensure that the multimode fiber would be embedded such that the bend radius of the fiber would match the minimum bend radius to maintain total internal reflection as recommended by the manufacturer. This value was specified as 120× the cladding diameter (125 μm). This peg spacing may have been chosen to match the specified minimum bend radius but the weave design

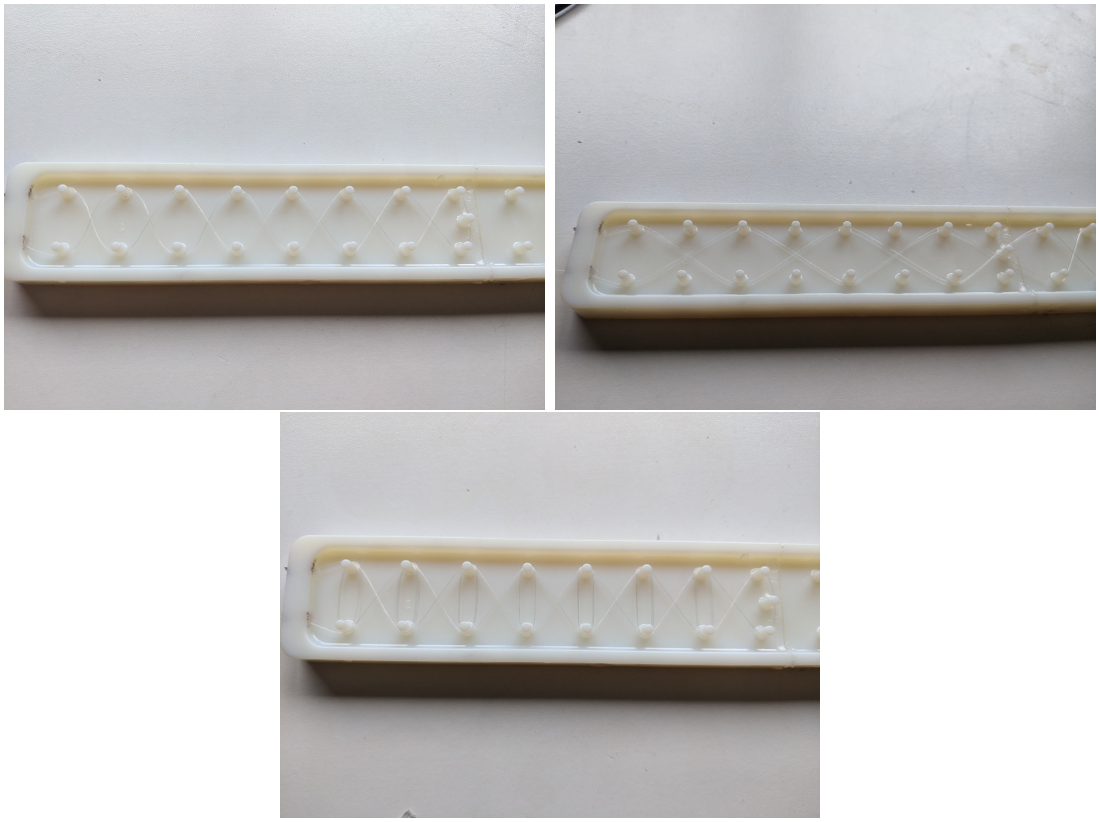

Figure 2.1: Left to Right, Top to Bottom: Single Weave, Half Weave, Double Weave, Pegs are Spaced 1.5 cm apart

of the fiber can be altered to modulate the intensity of macrobend losses. There were three weave patterns that were tested in this experiment, which are called single-, half-, and double-weaves. The single-woven fiber is simply wrapped around consecutive pegs, alternating sides each turn. The half-weave is exactly the same as this, only the fiber is wrapped around every other peg on alternating sides, resulting in a sinusoid with a spatial frequency of half of the single weave. The double-weave is the most complicated; it is first wrapped around a pair of pegs that are directly opposite each other, then wrapped around the next peg on the alternate side (the same way as in the single-weave) before being wrapped around both adjacent pegs again. The double weave will appear to have a single-woven fiber superimposed over fiber wrapped around adjacent pegs when completed. Each sensor is split into three sections, allowing it to measure the curvature

of three independent sections. One fiber will be embedded in the upper third of the mold only, one will be woven through the upper and middle thirds, while the last is woven through the entire length of mold. For the middle and lower sections of the sensor, the fibers are embedded with a half-weave until the fiber reaches its respective section, then is woven with either the single- or double-weave pattern. This allows the output of the fibers in the lower sections of the sensor to be minimally affected by bending in higher sections. Bending in higher sections will nevertheless cause some losses in the lower and middle fibers, although they are far more sensitive to bending losses in their respective section. The mold with woven fibers was filled with approximately 40 grams of Dragonskin 10 silicone and cured for a half hour at 70C. The cured sensor was allowed to cool, and then bonded to four stacked layers of adhesive-backed foam using Smooth-on Silpoxy. Having the sensor bonded to this foam substrate lifts it away from the neutral bending axis, which increases the amount of strain that experiences when bent. This allows for greater losses from the fibers embedded in the sensor, providing a greater demonstration of its capabilities.

2.2 Experimental Setup

This device uses motion capture for real-time ground truth measurement of the pose of the arm. The device was set up on a steel plate, to allow for the use of magnetic optical stands to secure the position of the lenses, coupling devices, and detector. The optical train consisted of a Helium Neon laser being directed into a collimating lens and coupling into three fibers at once. On the incident end, the fibers terminate into a ThorLabs CMOS camera that serves as the detector. The camera is controlled with the ThorCam software to record a series of TIF images that contain the fiber outputs on its aperture. The sensor was attached to a styrofoam board, a ziptie and some adhesive

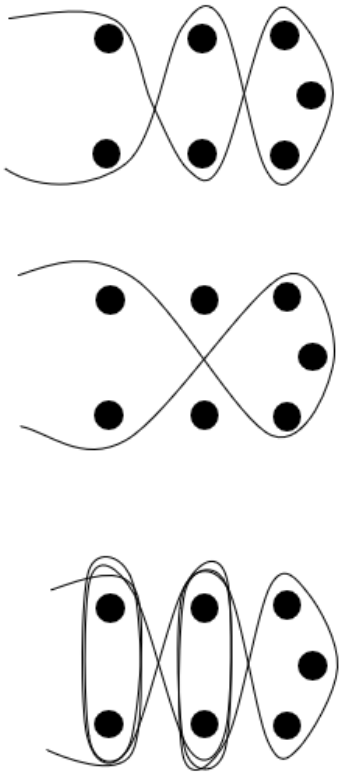

Figure 2.2: Sketch showing Single-, Half- and Double-weave

foam were used to secure the top section of the sensor in place, and limit the amount that the top face of the sensor can rotate (simulating a cantilever beam condition). 14 LED motion capture trackers were attached to the sensor body with adhesive-backed velcro. They were attached in pairs; with pairs being placed at the top, middle, and bottom of each of the thirds that the sensor was divided into. Arcs were drawn directly onto the styrofoam board corresponding to different sections along the sensor body, then holes were pressed into foam board using quarter inch screws.

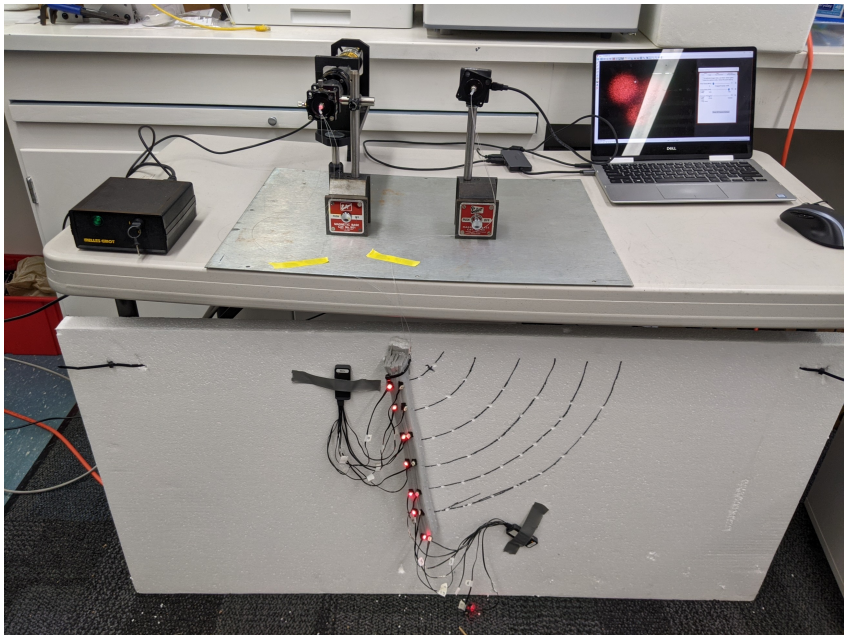

Figure 2.3: Set up showing optical train and soft sensor device with motion capture trackers, ThorCam running on PC

2.2.1 Coupling and Emitting Fixtures

In order to minimize the footprint and cost of the experimental setup, only one light source and detector were used in this experiment. 3D printed parts were designed for coupling the fibers with both the light source and the camera. These parts were fundamentally just short cylinders with an 1/8" outer diameter that fit snugly in an

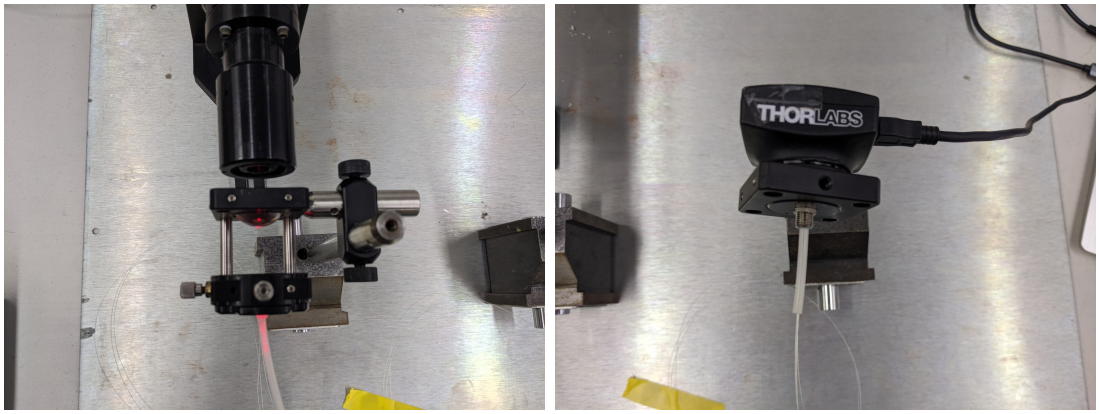

Figure 2.4: Light Source and Camera Coupling

SMA connector, with three small central holes that the optical fiber would go through. In Solidworks, these central holes were designed to have a larger diameter than the optical fiber (.5mm vs a .25mm diameter for the fiber used in this experiment) because the resolution limits of the Objet printer would not allow such a small hole to be well-formed. When they were printed, the holes were in fact smaller than the diameter of the optical fiber (3D Printers almost always undersize internal voids), but were large enough to serve as a pilot hole for a 250 micron diameter drillbit which allowed for a snug fit between the coupling device and the fibers.

Before drawing the fibers through the holes of the coupliong fixture, some plastic tubing with the approximate outer diameter of the coupling devices (about 3mm or 1/8") was placed over the fibers. Once the fibers had been drawn through both the plastic tubing and the 3D-printed coupling fixture, the assembly was bonded with superglue. A drop of superglue was placed where the fibers met the base of the 3D-printed part, and the plastic tubing was brought into contact with the back of the part. Then, drop of accelerant was placed at the joint and through the back end of the plastic tubing to cure the superglue and make the assembly rigid. Lastly, the excess fiber protruding from the end was cut flush with the end of the coupling fixtures with a carbide scribe. It is

important that the emitting end of the fixture be as close as possible to the aperture of the camera. Even with the multimode optical fiber which has a numerical aperture of 0.1, the light is dispersed enough that there is some overlap between the spots projected from each fiber. This is made worse with the PMMA fiber, for which the numerical aperture was not specified. This fiber is still much more sensitive to macrobend losses than the multimode fiber and was still chosen despite the outputs overlapping.

Figure 2.5: Light coming out of emitting fixture

The emitting end is simply cylindrical, so that the end of the coupling fixture can be pushed through the SMA connector that is threaded to the CMOS camera. This way, the fibers can be as close to the aperture as possible, preventing the outputs from spreading out to the point of overlapping and becoming indistinguishable.

The coupling end features a flange that comes out the back of the SMA connector that is aligned with the collimating lens. This makes it easier to rotate the fiber matrix, which can affect the amount of light entering each fiber. The SMA connector had variable vertical and horizontal position. These as well as the angle of rotation of the 3D printed fixture were tuned so that the light output at the emitting end were roughly equal.

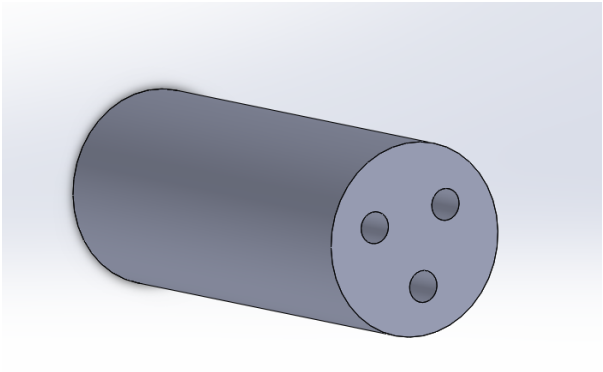

Figure 2.6: CAD Model of Emitting End

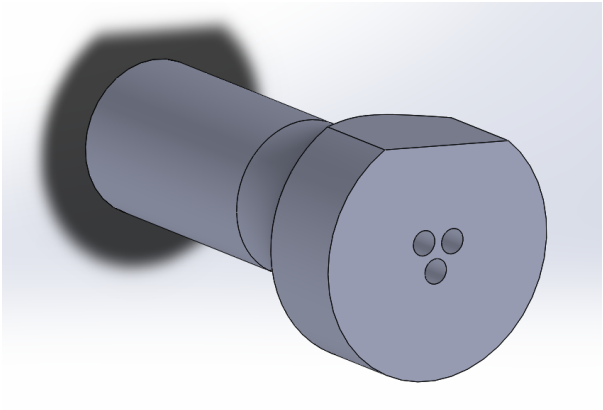

Figure 2.7: CAD model of Fixture for Coupling Light into Fibers

Chapter 3

Design of Experiment

3.1 Data Capture and Analysis

As stated above, the output of the three optical fibers coming out of the emitting end of the sensor are photographed directly using a CMOS camera. The images are saved as a time series of TIF files. A MATLAB script was written to analyze the information from the photographs. The photographs are converted to an array of gray scale values. By taking the gray scale data along a centerline through the fiber output spot and plotting it against the pixels position along the line, one can very clearly see that the light intensity follows a normal distribution from the central axis of the fiber. These data can be curve-fitted with MATLAB to fit a Gaussian profile. The peak of the Gaussian is the most prominent parameter that changes when subjected to bending but it can change in other ways as well. Below is an example of a high intensity and low intensity spot.

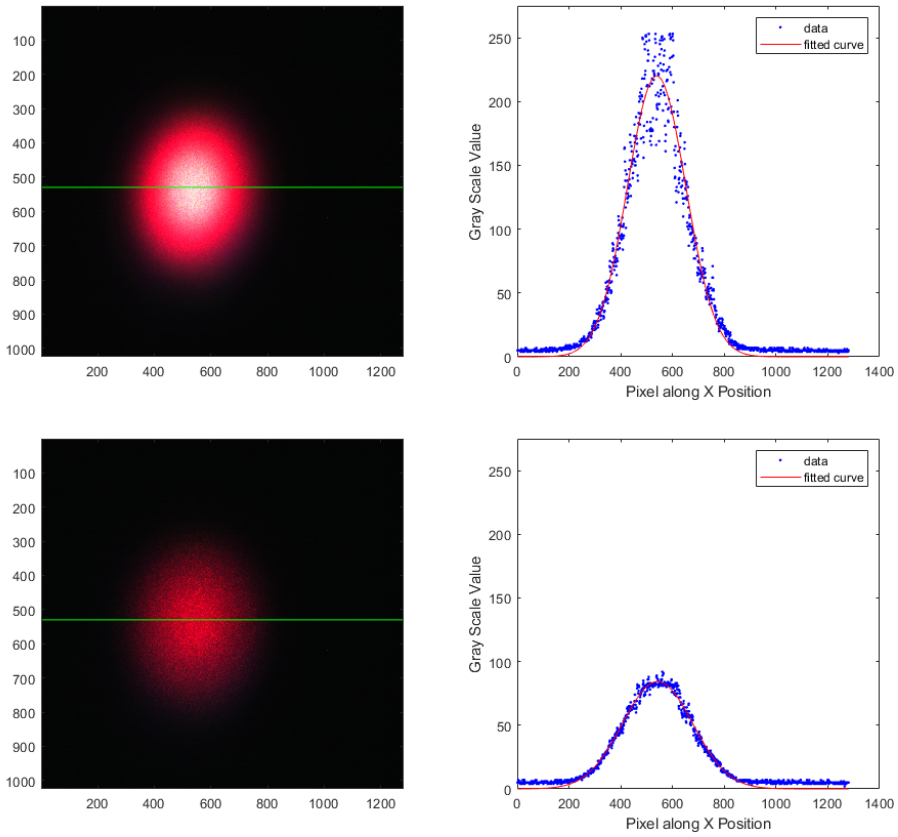

Figure 3.1: Bright and Dim Fiber Outputs, Single Fiber, Sampled Pixels Shown in Green

3.2 Fundamental Sensor Performance

The sensor outputs are affected by the location of the of the applied bending moment. If a moment is applied to the top third of the sensor, all three fibers are being compressed and therefore there should be attenuation in the signal of each of the fibers. The fiber that is woven only through the top third and not the others is woven with a higher frequency, therefore, the intensity loss measured from this fiber should be more severe than the outputs of the other two. An example of this is shown below in comparison with an unbent sensor. The top right spot corresponds to the fiber woven through the top section of the sensor. This is the least sensitive fiber to macrobend losses. The output change is difficult to discern in this case, which will be a matter of discussion of viability

of this sensor.

Similarly, if a bending moment is applied to the center third of the sensor, two fibers are being compressed, causing signal attenuation in the fibers woven through the center and bottom third only. It goes without saying, that a bending moment applied to the bottom third of the sensor only causes attenuation in that section. Examples showing the performance of the sensor when bent in each of its three principal sections, as well as an unbent baseline, are shown throughout this section along a photograph of the orientation. The outputs shown in the figures in this section were not directly analyzed, as it was at this point that it was noticed that the attenuation of the light in static poses was not as intense as it was during transient motion.

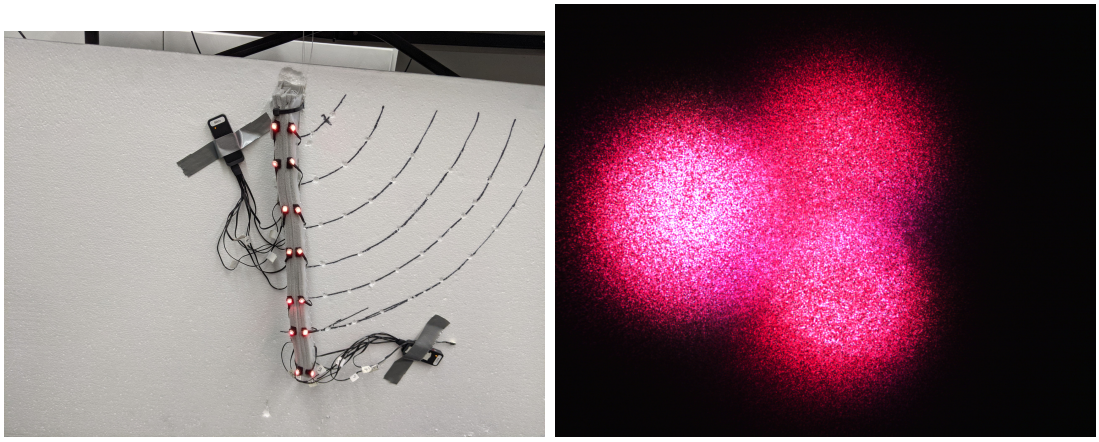

Figure 3.2: Unbent Sensor and Output

3.3 Experiment

An experimental procedure was designed so that the pose of the soft continuum sensor could be measured directly via motion capture and compared to the output of the fiber optic cables. Since the camera being used lacked an external trigger, once both the the camera and the motion capture system were recording, the trackers were hidden from

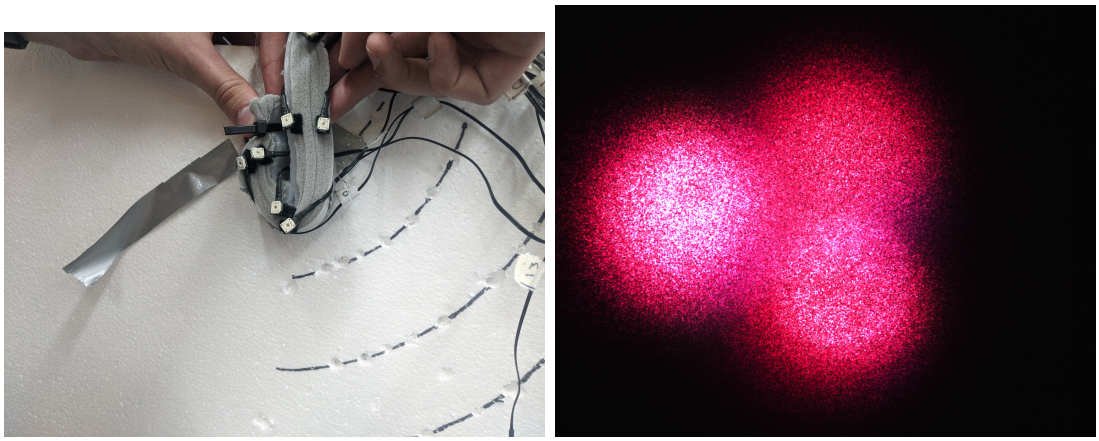

Figure 3.3: Bend in Top of Sensor and Output

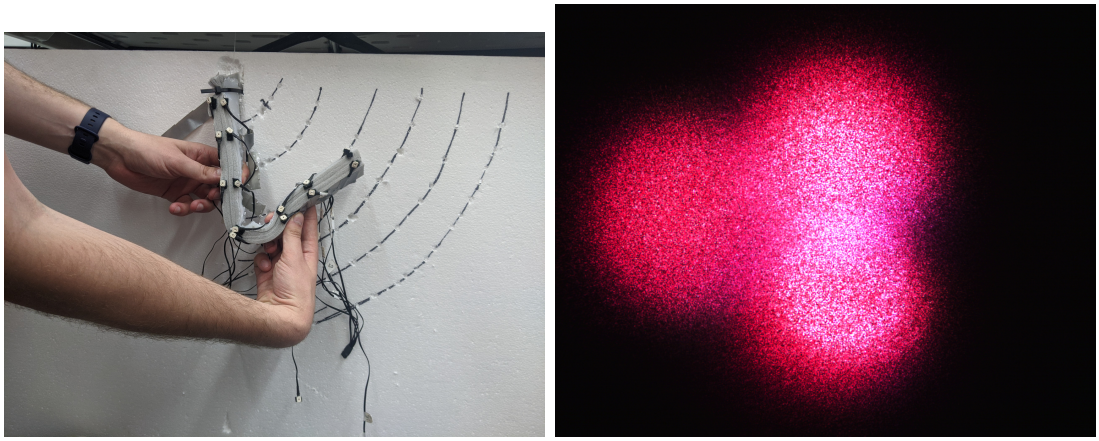

Figure 3.4: Bend in Middle of Sensor and Output

the motion capture cameras and the HeNe laser was shut off momentarily. The laser was restarted, and the trackers were uncovered as soon as the laser light showed up on the camera once again. This provides a visual cue for the user for synchronization between the two data streams. A more sophisticated synchronization should be used in future work, a camera that featured an external trigger could be easily integrated with motion capture. Once this was done, the soft continuum sensor was then manually manipulated. Screws were placed in the holes made in the foam board as the sensor was manipulated, being used to induce bending in specific sections of the sensor. Numerous different poses

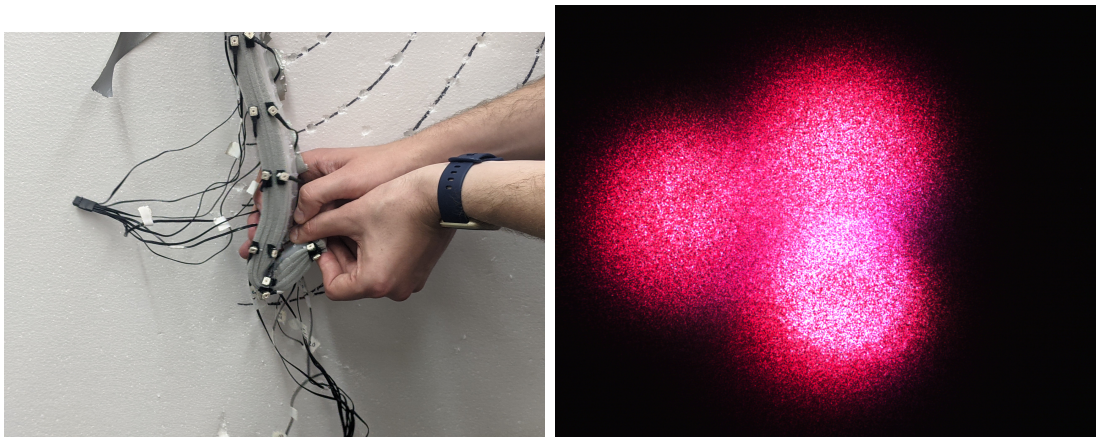

Figure 3.5: Bend in Bottom of Sensor and Output

were created using a number of screws in different positions along the arc lines. The data collected from the manipulating the sensor into different poses could hopefully constitute training data for a data-driven analysis approach such as a neural network.

Unfortunately, the sensitivity of the sensor during this experiment did not show appreciable sensitivity to bending as expected. The reasons for this are discussed in detail later on, but the primary reasons are the constraint conditions imposed on the sensor and substantially weaker signal attenuation for a statically deformed sensor than for one that is undergoing bending dynamically. Other potential reasons that the sensitivity may have been insufficient could be low exposure on the camera aperture and poor laser-fiber coupling, affecting the amount of light detected and transmitted respectively. Above is a comparison of two different frames showing minimal difference between the output power. These two images where pulled from an experiment where arbitrary poses where formed by manually manipulating the sensor into different shapes and holding it in place by putting screws into the styrofoam board. The frames in Figure 3.7 were taken approximately 2 minutes apart (tests lasted between 3 and 5 minutes), and a wide variety of shapes were achieved.

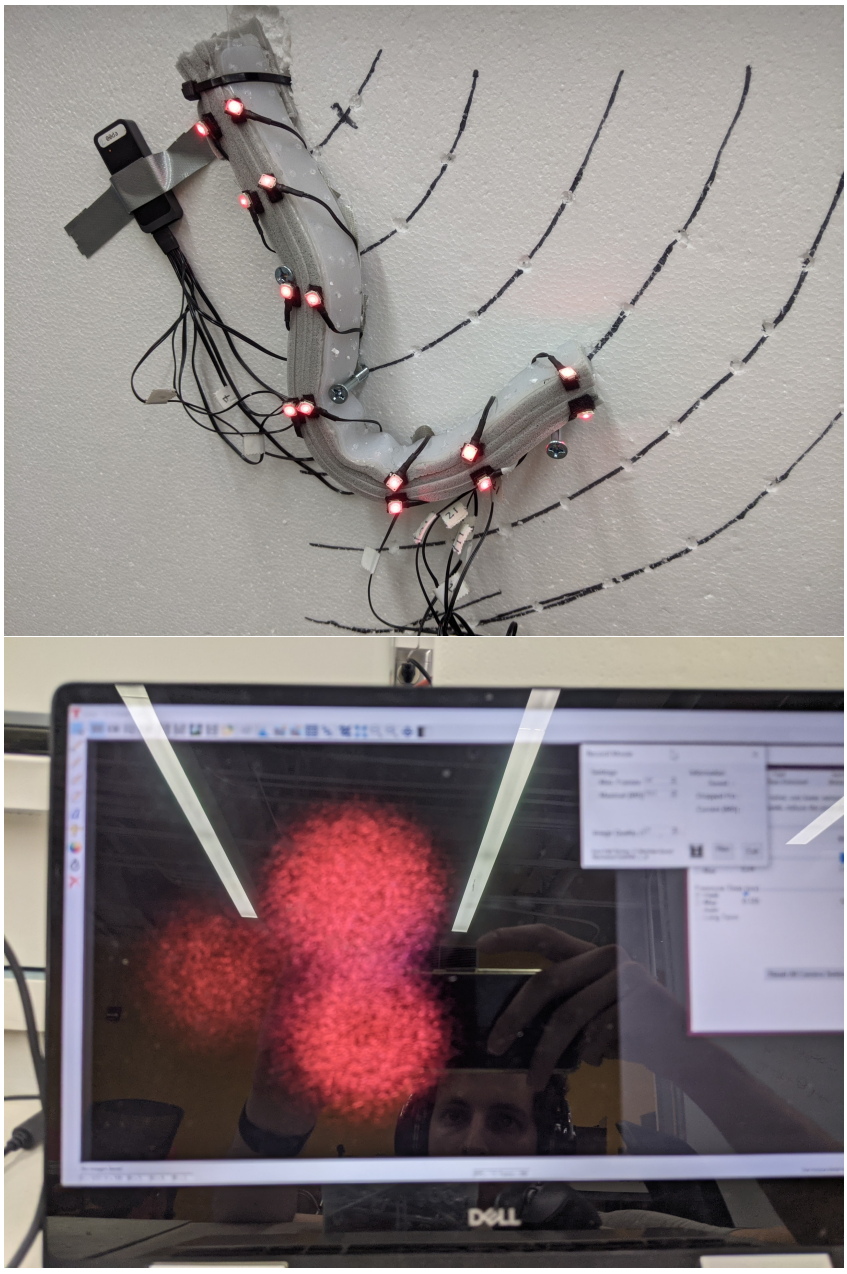

Figure 3.6: Sensor Manipulated into Arbitrary Pose with Corresponding Sensor Output On Camera

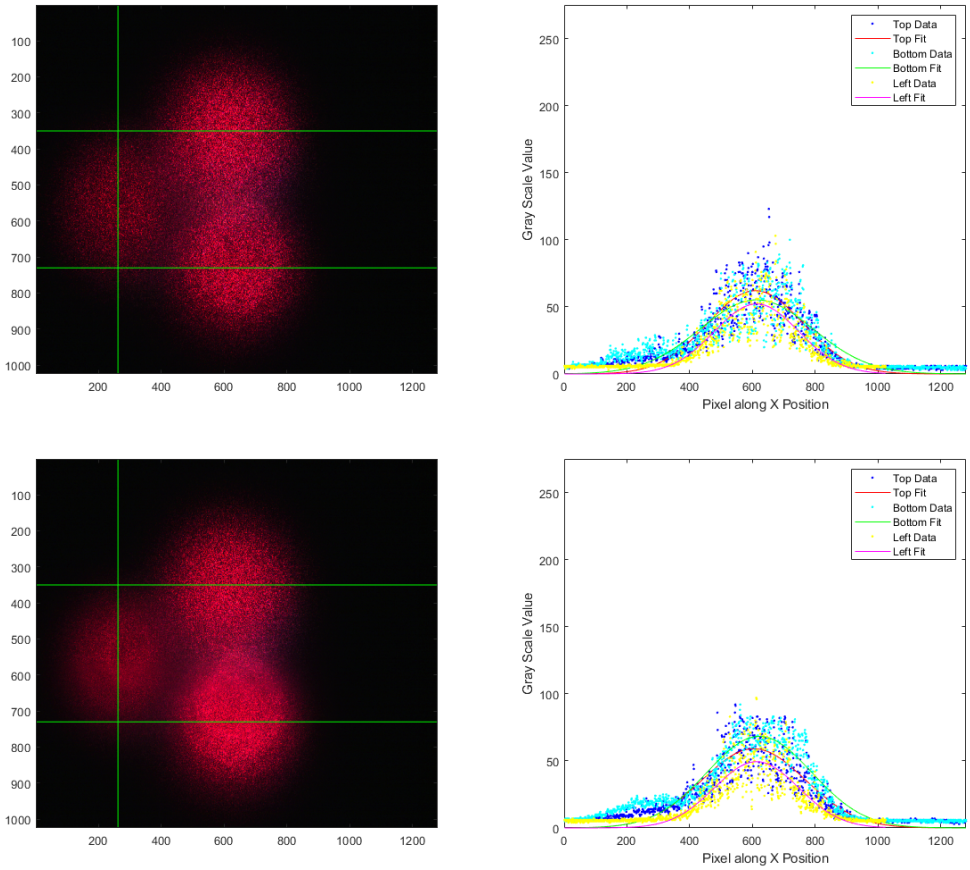

Figure 3.7: Sample Results from Experiment

Chapter 4

Results, Discussion, and Conclusion

Results and Discussions

The fiber optic sensor did not show strong attenuation in its signal when subjected to compound curvatures in the experiment. Interestingly, it appears that the attenuation in the signal is much more sensitive to manual bending than constraining the soft sensor to certain shapes using screws in the foam board. This could be for a number of reasons. One possible explanation is that the top of the soft sensor is not properly constrained. It was stated earlier that ideally that the top of the sensor should have a fixed end constraint, making it behave like a cantilever beam. This would maximize the amount of bending stress that the sensor would experience.

However, this device does not a have a proper cantilever end condition. The backside of the sensor is superglued to another piece of adhesive foam which is attached to the styrofoam, and additional support is created by looping a ziptie through the styrofoam board and securing it around the sensor. This constraint may sufficiently prevent rotation of the sensor in the vicinity of the styrofoam board, but the sensor is substantially thick that the torsion induced at the support causes the cross section of the sensor to twist,

especially as distance from the sensor-styrofoam interface is increased. This minimizes the bending stress throughout the sensor. This in effect causes the sensor constraint to resemble that of a pinned beam more so than a cantilever beam, explaining why the sensor in the experiment did not respond as it did when testing it by holding it at two different points and bending it manually. Future experiments should take measures to improve the quality of the cantilever condition applied to the top of the sensor.

The detector used was merely a single CMOS camera that captured the outputs of three embedded fiber optic cables. This was done because it was thought that perhaps the distribution of light being emitted from the fibers may have more information coded into them than simply the total light flux. There are numerous papers that do similar experiments as done here albeit with with photodiodes in place of the CMOS camera utilized in this case. One reason that it is attractive to use a camera for detection is that it makes very clear what exactly is happening to the light signal as the sensor is subjected to bending. However, under cursory analysis of individual rows of gray scale pixel values showed little change to any parameter other than the peak intensity of light. It still may hold true that there is independence between the parameters of a Gaussian fiber optic output (variance vs. peak intensity is the most obvious). A more robust analysis of the signal being projected onto the sensor would need to be done to determine this. Additionally, computer vision techniques would be well employed here. Another shortcoming of utilizing one camera is that there is limited space on the aperture to project the light being emitted. Overlap between the images makes parsing the data nontrivial. The coupling fixture for the emitting end should have holes that are spread farther apart, which is difficult because the coupling fixture is limited by the diameter of the SMA connector. A simple solution would be to use one camera for every fiber, but this is expensive and introduces plenty of its own problems. The data examined in this experiment were merely lines of pixels that intersected the dots corresponding

to each fiber optic cable. The primary problem here is that recording a time series of photographs uses an absolutely staggering amount of disk space, so only utilizing a small fraction of this data for analysis could be a missed opportunity. Using a camera as a detector would be a great idea if the entirety (or at least a substantial portion) of the data obtained can be used, otherwise it is much more prudent to simply use photodiodes to measure the light flux.

Constraining the sensor using screws presents a similar loading problem. The sensor is free to slide along the screw, which obviously constrains the sensor less than a pinned or fixed condition. When releasing the sensor after manipulating it into a certain position, restoring forces may cause translation along the screws, undoing some of the bending stress applied to the sensor. It is unlikely that that this affects the sensor output as much as the loading condition seen at the top of the sensor, but it may play a role nevertheless.

Other factors that could be contributing to the issues with this experiment is the the sensitivity of the sensor to transient effects and disturbances. When the sensor is being bent, the signal attenuates more during the bending phase, and then seems to be restored slightly if held in a static position. Signals may absolutely still be diminished while the sensor is bent in a static position, but the dominance of transient effects makes a simple correlation of signal strength to bend radius unfortunately difficult. This was not noticed until the experiment performed in this investigation was done, with preliminary experiments not showing this phenomenon as much. A possible explanation could be the signal to noise ratio being decreased by applying an unbalanced force to the sensor. In the case of the experiment performed, the signal was significantly noisier than in seen in figure 3.1. The case here could be that the noise was reduced during the transient motion, making the attenuation more clear, and then the noise returned during the static hold, making the attenuation more difficult to see and measure. A study that examines

more dynamic manipulation of a soft robot equipped with this sensor could be potentially insightful.

The sensor's behavior when subjected to unintended disturbances is also cause for concern. Touching or moving parts of the optical fibers that are not encapsulated can dramatically affect the output on the camera. The fibers were taped down to the table for this experiment so that the risk of them getting caught or wrapped on something was minimized but it nevertheless raises questions about the sensors robustness. When manipulating the sensor in ones hands, applying pressure to the fibers encapsulated in silicone also alters their output. The pressure causes contact between the overlapping fibers, and the output then tends to decrease in noise. There is a notable difference in the uniformity of the Gaussian fit before and after the sensor has been touched, even if no bending has occurred. During the compound curvature experiment, there is only ever pressure if a screw had been placed on the silicone side of the sensor, which only occurs if one of the sections is placed in tension rather than compression.

The last and most expedient issue that may have arisen in this experiment is simply poorly tuned camera settings. The sensor output is based on gray scale values of the image and is therefore highly dependent on the exposure time of the camera. This is a difficult thing to balance, as it is easy to overexpose the aperture and get saturated values, causing a plateau in the Gaussian fit. Likewise, an exposure time that is too low will limit the maximum output and by extension, the resolution of the sensor. Since the Gaussians seen in the time series analysis seldom reach values in excess of 100, it is recommended that the exposure time be increased.

The construction process of the sensor could also be improved. The most difficult part of fabrication is weaving the fiber through the mold. By weaving the fiber through the mold, some elastic energy is stored in the fiber. There were many times that the fiber sprung out of the mold and undid all of the weaving. If this occurred in a section where

more than one fiber lied, then the other ones would often be knocked out of place as well. This can be mitigated by pressing on the previous crossover during the weaving process each step of the way, as well as maintaining tension in the fibers that have already been threaded through the mold. A good way to do this is to tape down both ends of the fiber to the working surface after that fiber has been woven all the way through. An important property to note is that the fiber will be physically very close to the bottom of the mold when the silicone is case. After curing and removing the sensor from the mold, one should take note of what side the fiber is on. When attaching the sensor to something, the fiber side should be face down, as that way it is far less likely to break through the silicone and delaminate.

Conclusion

This experiment aimed to create a reliable, optics-based sensing solution for soft robotic platforms that can offer robust and reliable proprioceptive sensing at a fraction of the cost of a state-of-the-art system. The system developed attempted to take advantage of the optical intensity losses that are characteristic of fiber optics when they are bent below their minimum bend radius. While this principle was shown to be true in simple cases where the sensor was manually manipulated, as in figure 3.1 its reliability and versatility were put into question when subjected to compound curvatures and can be seen in figure 3.7. This likely has to do with the inadequate degree of constraint provided by the experimental setup. If this were to be attempted in the future, more robust constraints should be applied to the soft sensor. For example, if the whole end were to have a solid fixed constraint, and there were a series of supports that were fixed along the axis of the sensor that were free to move perpendicular to it, a wide variety of geometries simply by adjusting the later position of the supports. Another possibility would be

to have rods that are bonded to the back of the sensor, normal to the plane that the styrofoam board lies in figure 2.3. These rods could be placed in holes on some plane behind the sensor. In effect this is the same experiment as conducted in this paper, albeit with fixed constraints rather than ones that allow for translational motion between the sensor and supports.

This investigation unfortunately did not demonstrate fiber optic intensity modulation as a particularly viable shape-sensing solution for soft systems. The working principle was only minimally demonstrated. This does not mean that using optical intensity losses for correlation to the shape of a soft system is not an endeavor worth pursuing. The issues with this particular experiment were possibly caused by loading conditions that were used when testing the soft sensor, difficulties from not taking full advantage of using a camera as the detector of our system, and failure to take into account the dominance of transient effects and disturbances to the fiber optic cables over the attenuation caused by static bending. Any future investigations on using fiber optic intensity modulation for soft robotic systems that are able to mitigate these effects may very well succeed in creating in creating a reliable, low-cost proprioceptive sensing solution that could be deployed on a soft robotic platform. This investigation did manage to demonstrate a very reliable way of delivering light through a soft continuum. With some adjustments to the design it is not hard to imagine that embedded optical fibers could be used to deliver light to photo-activated pouch motor, serving as the basis of a light-actuated soft robot.

Bibliography

[1] D. A. Haggerty, M. J. Banks, P. C. Curtis, I. Mezić, and E. W. Hawkes, *Modeling, reduction, and control of a helically actuated inertial soft robotic arm via the koopman operator*, 2020.

[2] K. C. Galloway, Y. Chen, E. Templeton, B. Rife, I. S. Godage, and E. J. Barth., *Fiber optic shape sensing for soft robotics*, *Soft robotics, 6(5), 671–684.* (2019).

[3] M. Yang, Q. Liu, H. S. Naqawe, and M. P. Fok, *Movement detection in soft robotic gripper using sinusoidally embedded fiber optic sensor*, *Sensors* **20** (2020), no. 5.

[4] C. To, T. Hellebrekers, J. Jung, S. J. Yoon, and Y. lae Park, *A soft optical waveguide coupled with fiber optics for dynamic pressure and strain sensing*, in *Proceedings of (IROS) IEEE/RSJ International Conference on Intelligent Robots and Systems*, pp. 3821 – 3827, IEEE, October, 2018.

[5] S. S. et al, *Macrobend optical sensing for pose measurement in soft robot arms*, *Smart Mater. Struct* **24** (2015).

[6] K. Masuya, *Low-cost coil-shaped optical fiber displacement sensor for a twisted and coiled polymer fiber actuator unit*, *IEEE Robotics and Automation Letters* **5** (2020), no. 4.

[7] R. L. Truby, C. D. Santina, and D. Rus, *Distributed proprioception of 3d configuration in soft, sensorized robots via deep learning*, *IEEE Robotics and Automation Letters* **5** (2020), no. 2 3299–3306.